



HAL
open science

Reflection and transmission of solar light by clouds: asymptotic theory

A. A. Kokhanovsky, T. Nauss

► **To cite this version:**

A. A. Kokhanovsky, T. Nauss. Reflection and transmission of solar light by clouds: asymptotic theory. Atmospheric Chemistry and Physics, 2006, 6 (12), pp.5537-5545. hal-00296093

HAL Id: hal-00296093

<https://hal.science/hal-00296093>

Submitted on 18 Jun 2008

HAL is a multi-disciplinary open access archive for the deposit and dissemination of scientific research documents, whether they are published or not. The documents may come from teaching and research institutions in France or abroad, or from public or private research centers.

L'archive ouverte pluridisciplinaire **HAL**, est destinée au dépôt et à la diffusion de documents scientifiques de niveau recherche, publiés ou non, émanant des établissements d'enseignement et de recherche français ou étrangers, des laboratoires publics ou privés.

Reflection and transmission of solar light by clouds: asymptotic theory

A. A. Kokhanovsky¹ and T. Nauss²

¹Institute of Remote Sensing, University of Bremen, O. Hahn Allee 1, 28334 Bremen, Germany

²Laboratory of Climatology and Remote Sensing, Marburg University, Deutschhausstr. 10, 35032 Marburg, Germany

Received: 22 May 2006 – Published in Atmos. Chem. Phys. Discuss.: 31 August 2006

Revised: 2 November 2006 – Accepted: 30 November 2006 – Published: 11 December 2006

Abstract. The authors introduce a radiative transfer model CLOUD for reflection, transmission, and absorption characteristics of terrestrial clouds and discuss the accuracy of the approximations used within the model. A Fortran implementation of CLOUD is available for download. This model is fast, accurate, and capable of calculating multiple radiative characteristics of cloudy media including the spherical and plane albedo, reflection and transmission functions, absorptance as well as global and diffuse transmittance. The approximations are based on the asymptotic solutions of the radiative transfer equations valid at cloud optical thicknesses larger than 5.

While the analytic part of the solutions is treated in the code in an approximate way, the correspondent reflection function (RF) of a semi-infinite water cloud R_∞ is calculated using numerical solutions of the radiative transfer equation in the assumption of Deirmendjian's cloud C1 model. In the case of ice clouds, the fractal ice crystal model is used. The resulting values of R_∞ with respect to the viewing geometry are stored in a look-up table (LUT).

The results obtained are of importance for quick estimations of main radiative characteristics of clouds and also for the solution of inverse problems.

1 Introduction

Clouds occupy more than 60% of the sky at any given time and are main regulators of weather and climate. Because the study of cloud properties on a global scale is of significant importance, many satellite cloud retrieval algorithms have been developed over the past decades whereupon most of these are based on so-called Look-Up Tables (LUTs) for the reflection function of clouds (e.g. Nakajima and King,

Correspondence to: A. A. Kokhanovsky
(alexk@iup.physik.uni-bremen.de)

1990). Kokhanovsky et al. (2003) have proposed an algorithm which is based on the analytical asymptotic solutions of the radiative transfer equations valid for optically thick clouds with a cloud optical thickness τ larger than approximately 5 and a single scattering albedo ω_0 larger than 0.98. Since the latter property limits the application to weakly absorbing clouds, we propose a new technique to overcome the limitation of small values of ω_0 which is of special importance for ice cloud remote sensing when the size of the scattering particles and therefore the absorption of radiation in the cloud can be quite large. Moreover, the 3.6 to 3.9 μm channels available on many satellite sensors are no longer excluded from the potential range of applications.

The new technique is based on simple equations that can be used for approximate analytical calculations of the reflection functions and light fluxes in cloudy atmospheres. Therefore, they enable the simplification of existing satellite and ground-based cloud retrieval algorithms while errors in the computation of the reflection function are generally smaller than errors related to uncertainties in the forward model and errors due to calibration uncertainties of optical instruments.

In the following section, a system of equations that accounts for multiple light scattering is presented, which can be used for the forward modeling of cloud optical properties. The accuracy of these analytical equations with respect to cloud reflection and transmission characteristics is discussed in Sect. 3.

The presented results can be used for the rapid estimates of various radiative cloud characteristics and also for the speeding up cloud retrieval algorithms.

2 General equations

It is well known that reflection $R_A(\mu_0, \mu, \phi)$ and transmission $T_A(\mu_0, \mu)$ functions of optically thick homogeneous plane-parallel light scattering layers over a Lambertian

surface with albedo A can be presented in the following analytical forms (van de Hulst, 1980; Kokhanovsky, 2006):

$$R_A(\mu_0, \mu, \phi) = R(\mu_0, \mu, \phi) + \frac{At_d(\mu_0)t_d(\mu)}{1 - Ar_s},$$

$$R(\mu_0, \mu, \phi) = R_\infty(\mu_0, \mu, \phi) - T(\mu_0, \mu)e^{-k\tau}, \quad (1)$$

$$T_A(\mu_0, \mu) = T(\mu_0, \mu) + \frac{At_d(\mu_0)r_p(\mu)}{1 - Ar_s},$$

$$T(\mu_0, \mu) = \frac{me^{-k\tau}}{1 - l^2e^{-2k\tau}}K(\mu_0)K(\mu). \quad (2)$$

Here $R \equiv R_A (A=0)$, $T \equiv T_A (A=0)$, the pair (μ_0, μ) gives the cosines of the incidence and observation angles, ϕ is the relative azimuth, $t_d(\mu_0)$ is the diffuse transmittance of a layer under illumination along the direction $\vartheta_0 = \arccos(\mu_0)$, r_s is the spherical albedo, $r_p(\mu)$ is the plane albedo for the diffuse illumination conditions and an observation along the direction specified by the viewing zenith angle $\vartheta = \arccos \mu$. $R_\infty(\mu_0, \mu, \phi)$ is the reflection function of a semi-infinite scattering layer having the same local optical characteristics (e.g., the same single scattering albedo ω_0 and the same phase function $p(\theta)$ with scattering angle θ) as the finite layer currently under study. The functions $r_p(\mu)$, $t_d(\mu)$ and r_s are defined as

$$r_p(\mu) = 2 \int_0^1 \bar{R}(\mu_0, \mu)\mu_0 d\mu_0,$$

$$t_d(\mu) = 2 \int_0^1 \bar{T}(\mu_0, \mu)\mu_0 d\mu_0,$$

$$r_s = 2 \int_0^1 r_p(\mu)\mu d\mu, \quad (3)$$

with $\bar{R}(\mu_0, \mu) = \frac{1}{2\pi} \int_0^{2\pi} R(\mu_0, \mu, \phi) d\phi$ and

$\bar{T}(\mu_0, \mu) = \frac{1}{2\pi} \int_0^{2\pi} T(\mu_0, \mu, \phi) d\phi$. The constants (k, l, m)

and the escape function $K(\mu)$ do not depend on τ and can be obtained from the solution of integral equations as described by van de Hulst (1980), Wauben (1992), and Kokhanovsky (2006). Expressions for $r_{pA}(\mu)$, $t_{dA}(\mu)$ and r_{sA} for arbitrary surface albedo values A can be derived from Eqs. (1), (2) with account for the definitions in Eq. (3). Namely it follows:

$$r_{pA}(\mu) = r_p(\mu) + \frac{At^2K(\mu)}{n(1 - Ar_s)},$$

$$r_p(\mu) = r_{p\infty}(\mu) - ltn^{-1}K(\mu)e^{-k\tau}, \quad (4)$$

$$r_{sA} = r_s + \frac{At^2}{1 - Ar_s},$$

$$r_s = r_{s\infty} - lte^{-k\tau}, \quad (5)$$

$$t_{dA}(\mu) = t_d(\mu) + \frac{Attr_p(\mu)}{1 - Ar_s},$$

$$t_d(\mu) = tn^{-1}K(\mu), \quad (6)$$

where t is the global transmittance defined by (see Eqs. 2, 3)

$$t \equiv 2 \int_0^1 t_d(\mu)\mu d\mu = \frac{mn^2e^{-k\tau}}{1 - l^2e^{-2k\tau}} \quad (7)$$

and

$$n = 2 \int_0^1 K(\mu)\mu d\mu. \quad (8)$$

Note that it follows from Eqs. (3) and (6–8):

$$t_A = \frac{t}{1 - Ar_s}. \quad (9)$$

A summary of the main equations can be found in Table 1.

The radiative characteristics $r_p(\mu)$, $t_d(\mu)$, r_s , t as well as $R(\mu_0, \mu, \phi)$ and $T(\mu_0, \mu)$ can be measured directly. Therefore, equations shown above can be of importance for the interpretation of correspondent experiments. For the use of the analytical Eqs. (1), (2), (4–7), (9) at arbitrary ω_0 and $p(\theta)$, several parameters ($k, l, m, n, r_{s\infty}$) and also functions $K(\mu)$, $R_\infty(\mu_0, \mu, \phi)$ and $r_{p\infty}(\mu)$ have to be derived. The problem is simplified when $\omega_0=1$. Then it follows: $k=m=0, l=n=r_{s\infty}=r_{p\infty}(\mu)=1$. For the general case parameters $k, l, m, n, r_{s\infty}$ can be parameterized as follows (van de Hulst, 1974; King and Harshvardan, 1986):

$$k = \left(\sqrt{3}s - \frac{(0.985 - 0.253s)s^2}{6.464 - 5.464s} \right) (1 - \omega_0g), \quad (10)$$

$$l = \frac{(1-s)(1-0.681s)}{1+0.792s}, \quad (11)$$

$$m = (1 + 1.537s) \ln \left(\frac{1 + 1.8s - 7.087s^2 + 4.74s^3}{(1 - 0.819s)(1 - s)^2} \right), \quad (12)$$

$$n = \sqrt{\frac{(1-s)(1+0.414s)}{1+1.888s}}, \quad (13)$$

$$r_{s\infty} = \frac{(1-s)(1-0.139s)}{1+1.17s}, \quad (14)$$

where

$$s = \sqrt{\frac{1 - \omega_0}{1 - \omega_0g}} \quad (15)$$

is the similarity parameter and

$$g = \frac{1}{4} \int_0^\pi p(\theta) \sin(2\theta) d\theta \quad (16)$$

Table 1. Radiative transfer characteristics of optically thick layers.

Radiative characteristic	$A=0$	$A \neq 0$
Transmission function	$T(\mu_0, \mu) = tn^{-2} K(\mu_0) K(\mu)$	$T_A(\mu_0, \mu) = tn^{-2} K(\mu_0) K(\mu) + \frac{Atn^{-1}K(\mu_0)r_d(\mu)}{1-Ar_s}$
Diffuse transmittance	$t_d(\mu) = tn^{-1} K(\mu)$	$t_{dA}(\mu) = tn^{-1} K(\mu) + \frac{At r_p(\mu)}{1-Ar_s}$
Global transmittance	$t = \frac{mn^2 e^{-k\tau}}{1-l^2 e^{-2k\tau}}$	$t_A = \frac{mn^2 e^{-k\tau}}{(1-l^2 e^{-2k\tau})(1-Ar_s)}$
Reflection function	$R(\mu_0, \mu, \phi) = R_\infty(\mu_0, \mu, \phi) - ltn^{-2} K(\mu_0) K(\mu) e^{-k\tau}$	$R_A(\mu_0, \mu, \phi) = R_\infty(\mu_0, \mu, \phi) - ltn^{-2} K(\mu_0) K(\mu) e^{-k\tau} + \frac{At^2 n^{-2} K(\mu_0) K(\mu)}{1-Ar_s}$
Plane albedo	$r_p(\mu) = r_{p\infty}(\mu) - ltn^{-1} K(\mu) e^{-k\tau}$	$r_{pA} = r_{p\infty}(\mu) - ltn^{-1} K(\mu) + \frac{At^2 n^{-1} K(\mu)}{1-Ar_s}$
Spherical albedo	$r_s = r_{s\infty} - lte^{-k\tau}$	$r_{sA} = r_{s\infty}(\mu) - lte^{-k\tau} + \frac{At^2}{1-Ar_s}$

is the asymmetry parameter.

Functions $K(\mu)$, $R_\infty(\mu_0, \mu, \phi)$ and $r_{p\infty}(\mu)$ can not be parameterized in terms of the similarity parameter alone. Therefore, LUTs of $K(\mu)$ for different values of μ and ω_0 have been calculated using the Heney-Greenstein phase function (van de Hulst, 1980) with an asymmetry parameter $g=0.85$ that is typical for water clouds. This can be done since both functions $K(\mu)$ and $r_{p\infty}(\mu)$ show only a weak dependence on the phase function and even on g for a fixed value of the similarity parameter (Kokhanovsky, 2006). For these calculations, a radiative transfer code developed by Wauben (1992) has been used which is based on van de Hulst's asymptotic fitting technique (van de Hulst, 1980). The LUT for $r_{p\infty}(\mu)$ has been prepared for a wavelength of $0.65 \mu\text{m}$ and Deirmendjian's cloud C1 model phase function (Kokhanovsky, 2006) using a radiative transfer code developed by Mishchenko et al. (1999). The final LUTs are represented in terms of μ and s so they can be applied at arbitrary values of g and ω_0 . Due to the reciprocity principle (van de Hulst, 1980), functions $K(\mu)$ and $r_{p\infty}(\mu)$ are identical to $K(\mu_0)$ and $r_{p\infty}(\mu_0)$ for the media under consideration.

The system of equations and LUTs specified above can be used to calculate all radiative properties of an optically thick layer except $R(\mu_0, \mu, \phi)$. In order to compute $R(\mu_0, \mu, \phi)$, the reflection function of a semi-infinite layer $R_\infty(\mu_0, \mu, \phi)$ must be determined. It depends on three angular parameters and also on the single scattering albedo and the phase function. Values of $R_\infty(\mu_0, \mu, \phi)$ enter the code through look-up tables that have been computed for the wavelength $\lambda=0.65 \mu\text{m}$ and different values of the single scattering albedo using the code developed by Mishchenko et al. (1999). A fixed gamma particle size distribution $f(a) = Ma^6 \exp(-1.5a)$ with an effective radius of $6 \mu\text{m}$ (ratio of the third to the second moment of $f(a)$) has been assumed; a is the radius of the particles and $M=3^5/(2^4 \times 5^8)$

is a normalization constant $\left(\int_0^\infty f(a) da = 1 \right)$. For the wavelength of $\lambda=0.65 \mu\text{m}$, a refractive index of 1.330683 has been chosen (Kokhanovsky, 2006) resulting in an asymmetry parameter equal to 0.85.

For ice clouds, the LUT for $R_\infty(\lambda=0.65 \mu\text{m})$ is based on the fractal model of scatterers for the phase function described by Mishchenko et al. (1999). A refractive index of 1.311 has been assumed, which leads to an asymmetry parameter of $g=0.7524$ for irregular fractal particles. Due to the large values of a_{ef} for ice crystals, the pre-computed LUTs are almost insensitive to the wavelength used for their calculations.

A Fortran code (CLOUD) performing all calculations according to the equations given above as well as all necessary LUTs can be downloaded from the internet <http://www.iup.physik.uni-bremen.de/~alexk>. The code is fast, reliable, easy to use, and accurate and therefore enables a rapid estimation of various cloud radiative transfer characteristics.

3 The accuracy of approximations

3.1 Diffuse light characteristics

The accuracy of the approximations for the plane albedo r_p , the diffuse transmittance t_d , and the diffuse absorptance $a_d=1-r_p-t_d$ is shown in Figs. 1–5 obtained using the exact radiative transfer code SCIATRAN (Rozanov et al., 2005) for a typical water cloud phase function calculated at $\lambda=0.65 \mu\text{m}$ and the particle size distribution described above.

Let us consider the obtained results in more details. First of all, one can see that the approximate equations describe the correspondent physical dependencies correctly. It follows

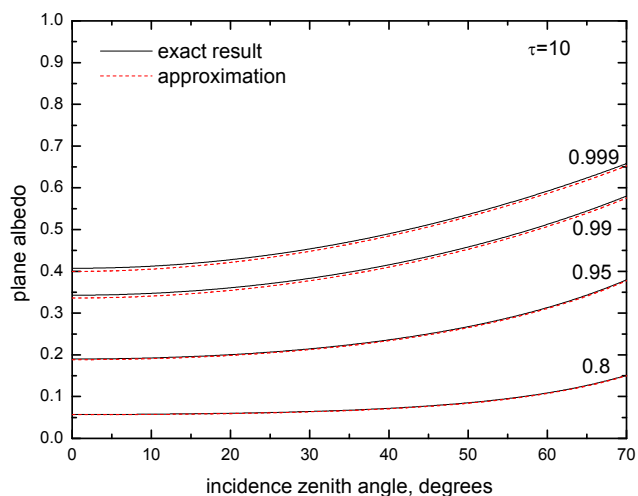


Fig. 1a. Dependence of the plane albedo on the incidence zenith angle for several values of the single scattering albedo and an optical thickness of 10. Exact results are given by black lines. Approximate results are given by red broken lines.

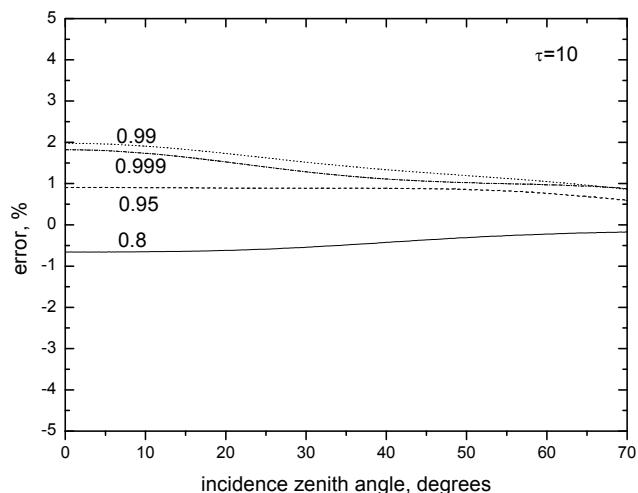


Fig. 1b. Relative error δ between the approximated values of the plane albedo as a function of the incidence zenith angle obtained from data shown in Fig. 1a.

from Fig. 1a that the plane albedo increases with the incident zenith angle ϑ_0 while the diffuse transmittance (Fig. 2) decreases. The reason for this is quite obvious. Light entering the medium under grazing angles has more chances to escape from the medium at the illuminated side. Interestingly, the diffuse absorptance (Fig. 3) is only weakly influenced by the light source angular position. The relative error $\delta = 100(1 - x_a/x_e)$ (x_a is the approximate value and x_e is the exact result derived from SCIATRAN) is very small. For the plane albedo it is smaller than 2% at $\tau = 10$ and $\omega_0 \geq 0.8$ (see

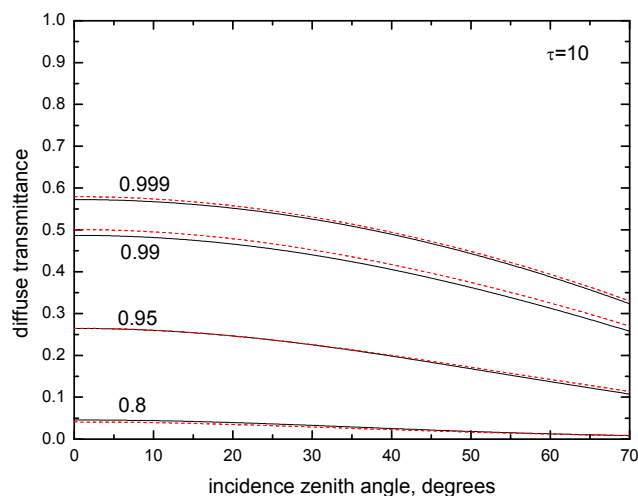


Fig. 2. The same as in Fig. 1a except for the diffuse transmission.

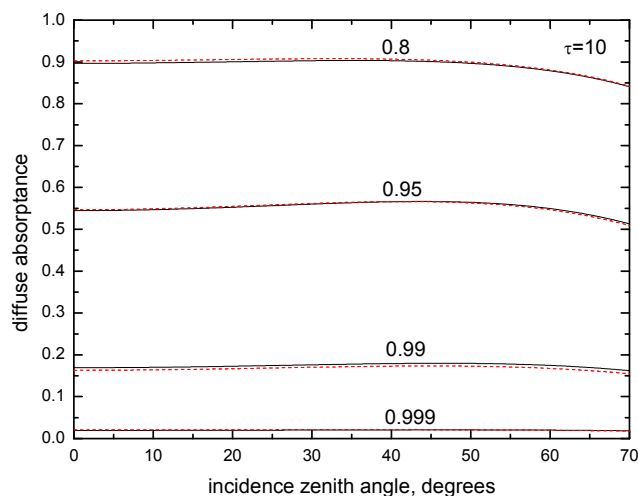


Fig. 3. The same as in Fig. 1a except for the diffuse absorptance.

Fig. 1b). The correspondent δ for the diffuse transmittance is somewhat larger. It can reach 12% at $\omega_0 = 0.8$. However, errors are smaller than 6% for values of the single scattering albedo larger than 0.95 and $\tau \geq 3$. Such an error of the diffuse transmittance will be translated to a much smaller error for the reflection function given by Eq. (1) due to the small influences of the surface term on the satellite signal in the case of thick clouds considered in this study. The error in a_d is smaller than 8% at $\omega_0 \geq 0.8$ and it is smaller than 5% at $\omega_0 \geq 0.95$. Consequently, equations given above can also be used for the estimation of the absorption and heating rates in cloud fields over underlying surfaces with varying albedos.

Figure 4a clearly shows that the approximation for the plane albedo r_p can be used for clouds with $\tau \geq 3$ with errors smaller than 5% (see Fig. 4b). For smaller values of τ , the theory given above is not applicable. It follows from Fig. 4a

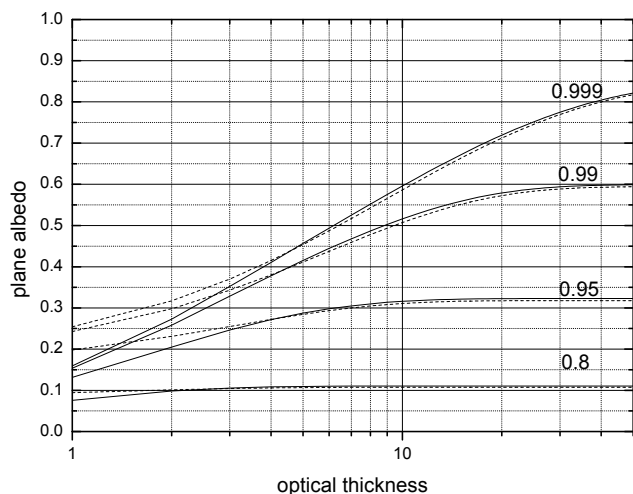


Fig. 4a. The same as in Fig. 1a except as a function of the optical thickness for a solar zenith angle of 60° . Approximate results are given by broken lines. Results obtained using SCIATRAN are represented by solid lines.

that the limit of the semi-infinite medium is reached at $\tau=5$ for a single scattering albedo equal to 0.8 (and, therefore, also at $\omega_0 < 0.8$).

The diffuse transmittance and also the diffuse absorptance calculated with the exact and approximate equations are shown in Fig. 5a as a function of the optical thickness. As one might expect the transmittance decreases and the absorptance increases with τ . These physical dependencies are well represented by equations shown above at least till $\omega_0=0.8$ and the errors are generally smaller than 10% (see Figs. 5b, c). Comparatively large errors for t_d at $\omega_0=0.8$ are due to the fact that $t_d \ll 1$ in this case.

Equations for r_p and t_d are simplified at $\omega_0=1$. Then it follows (Kokhanovsky, 2006):

$$r_p = 1 - t_d, \quad t_d = \frac{K_0(\mu_0)}{1.072 + 0.75\tau(1-g)}. \quad (17)$$

where $K_0(\mu_0) \equiv K(\mu_0, \omega_0=1)$. The accuracy of Eqs. (17) is studied in Figs. 6, 7 for the same phase function as has been used above and assuming that (Kokhanovsky, 2006)

$$K_0(\mu_0) = \frac{3}{7}(1 + 2\mu_0). \quad (18)$$

This equation gives the parameterization of the correspond LUT at $\omega_0=1$ and $\mu_0 \geq 0.2$.

The analysis of Figs. 6–7 shows that the simple Eq. (17) can be used for the computation of r_p and t_d with an error smaller than 5% at $\tau \geq 7$ and $\tau \geq 5$ respectively. For both parameters, the error is smaller than 1% at $\tau \geq 10$, $\omega_0=1$.

It is evident that errors for the pair (r_s, t) are even smaller than those for r_p and t_d . This is mostly due to the fact that one more integration is involved in the definition of (r_s, t) as

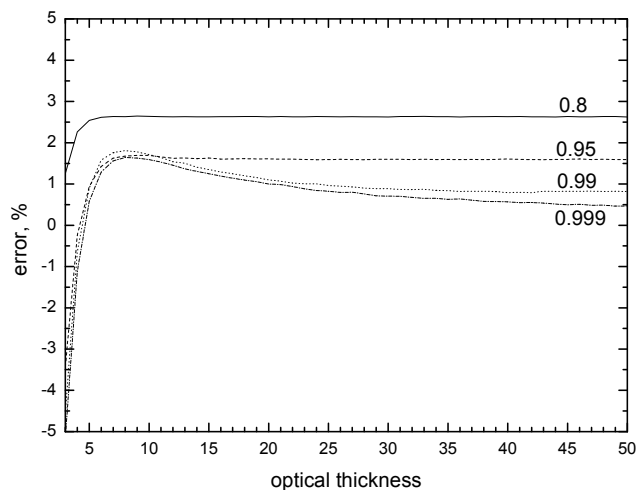


Fig. 4b. Errors calculated using data shown in Fig. 4a.

compared to (r_p, t_d) . In particular, we have found that the error of the asymptotic theory is smaller than 2% at $\tau \geq 3$ for r_s and it is smaller than 5% at $\tau \geq 5$ for t at $g=0.85$. The error decreases further with cloud optical thickness.

3.2 Reflection function

The accuracy of Eqs. (1), (2) is studied in Fig. 8 for $A=0$ and several values of ω_0 for the same phase function as above ($g=0.85$). Equations (1), (2) are transformed to the following forms at $\omega_0=1$:

$$R_A(\mu_0, \mu, \phi) = R(\mu_0, \mu, \phi) + \frac{At_d(\mu_0)t_d(\mu)}{1 - Ar_s}, \quad (19)$$

$$R(\mu_0, \mu, \phi) = R_{\infty 0}(\mu_0, \mu, \phi) - T(\mu_0, \mu),$$

$$T_A(\mu_0, \mu) = T(\mu_0, \mu) + \frac{At_d(\mu_0)r_p(\mu)}{1 - Ar_s}, \quad (20)$$

$$T(\mu_0, \mu) = tK_0(\mu_0)K_0(\mu), \quad (20)$$

where $R_{\infty 0}(\mu_0, \mu, \phi) \equiv R_{\infty}(\mu_0, \mu, \phi, \omega_0=1)$ and

$$t = \frac{1}{1.072 + 0.75\tau(1-g)} \quad (21)$$

is the global transmittance at $\omega_0=1$. Due to the conservation of energy principle it follows for the spherical albedo of non-absorbing media: $r_s=1-t$.

The comparison of exact and approximate results for a nadir observation and solar zenith angles ranging from 0 to 85 degrees is shown in Fig. 8 for the special case of a black underlying surface. It follows that the approximations and exact results are very close to each other at $\omega_0 > 0.8$ (the relative error is smaller than 2%). Smaller values of ω_0 are not typical for cloudy media in the visible and near-infrared. The high accuracy of the expression for R confirms that the value

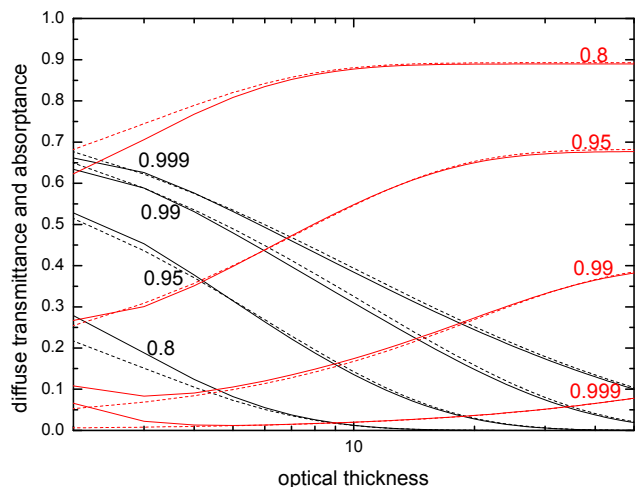


Fig. 5a. Dependence of the diffuse transmittance (black lines) and absorbance (red lines) on the optical thickness for several values of the single scattering albedo and an incidence zenith angle of 60° . Approximate results are given by broken lines.

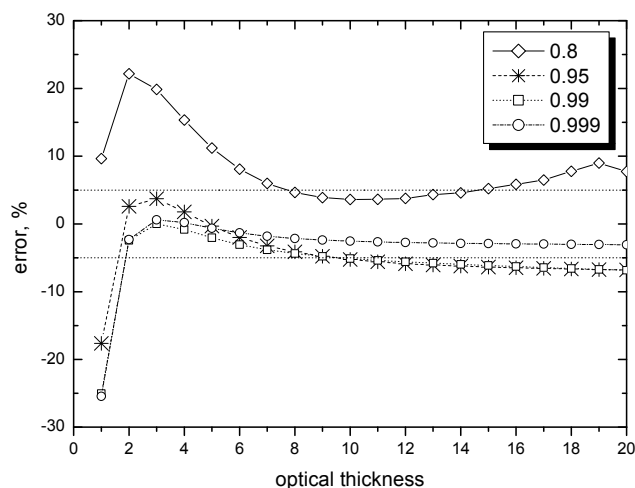


Fig. 5b. Errors in t_d calculated using data shown in Fig. 5a.

of $T = [R_\infty(\mu_0, \mu, \phi) - R(\mu_0, \mu, \phi)]l^{-1}e^{k\tau}$ is also calculated accurately in the framework of the approximation considered here.

Another interesting aspect is the behavior of the approximations for non-nadir observations. The results of calculations for an observation angle of 60 degrees and several azimuth angles are shown in Fig. 9. One can see that the approximation is capable to describe the case of non-nadir observations. For instance, the glory seen on the exact curve at an azimuth of 180 degrees is well reproduced by the approximation. Errors are below 0.5% for the case shown in Fig. 9.

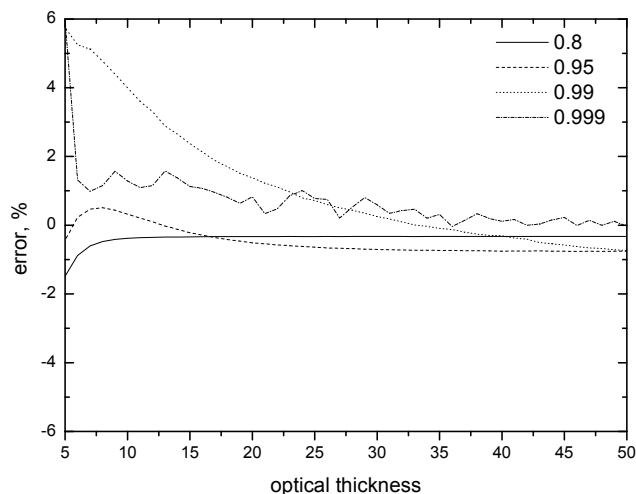


Fig. 5c. Errors in a_d calculated using data shown in Fig. 5a.

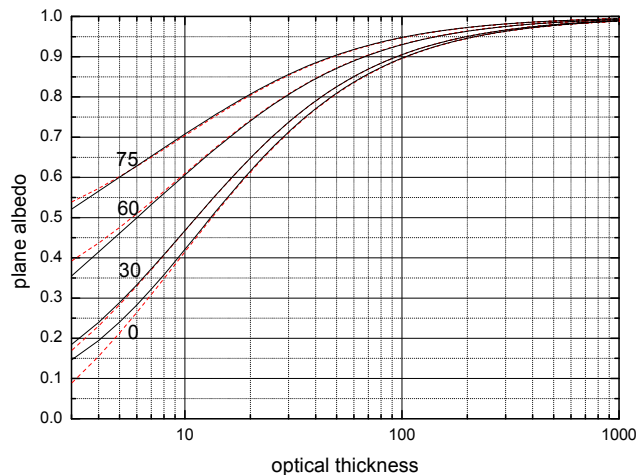


Fig. 6a. Dependence of the plane albedo on the optical thickness for several solar angles and $\omega_0=1$ according to exact results (black lines) and approximations (red lines).

Clearly, errors increase for smaller τ . This is shown in Fig. 10. However, they remain smaller than 5% at $\tau \geq 5$ (see Fig. 10b) and smaller than 1% at $\tau \geq 10$ and $\omega_0 \geq 0.8$. Smaller values of ω_0 are of no interest because such low values are not characteristic for water clouds in the visible and near-infrared. Interestingly, the approximation errors decrease with $\beta=1-\omega_0$ for a given τ . In particular, the code can be used with an error smaller than 5% at $\tau \geq 2$ and $\omega_0=0.8$ and errors are smaller than 5% at $\tau \geq 3$ and $\omega_0 \leq 0.95$. For non-absorbing clouds, the errors are smaller than 5% at $\tau \geq 5$ (see Fig. 10b).

All results shown above have been obtained for the case of clouds with droplet size distributions having an effective radius $6 \mu\text{m}$. It is of importance to see how the equations

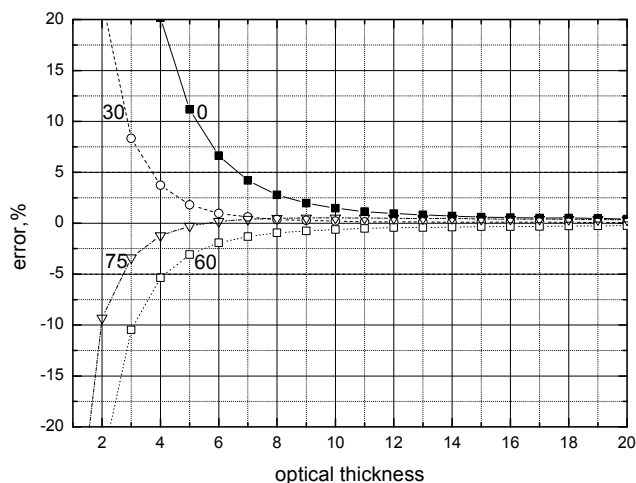


Fig. 6b. Errors calculated using data shown in Fig. 6a.

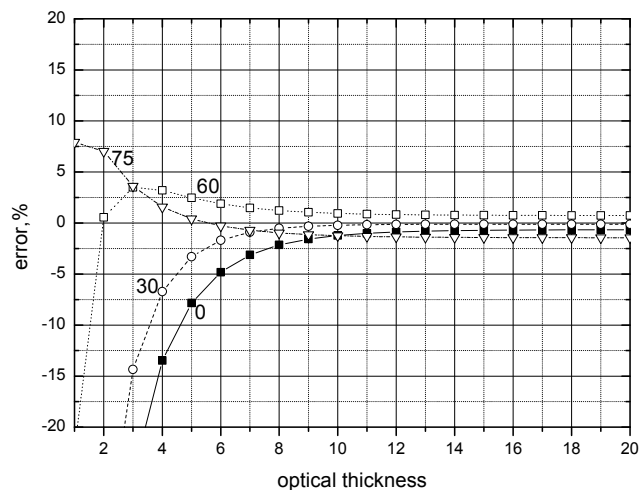


Fig. 7b. Errors calculated using data shown in Fig. 7a.

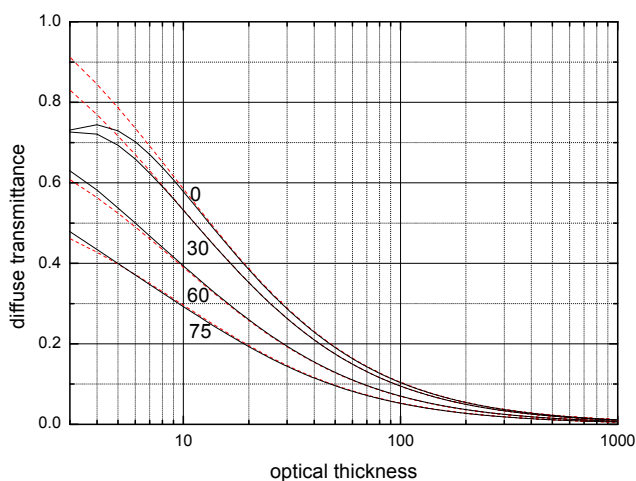


Fig. 7a. The same as in Fig. 6a except for the diffuse transmittance.

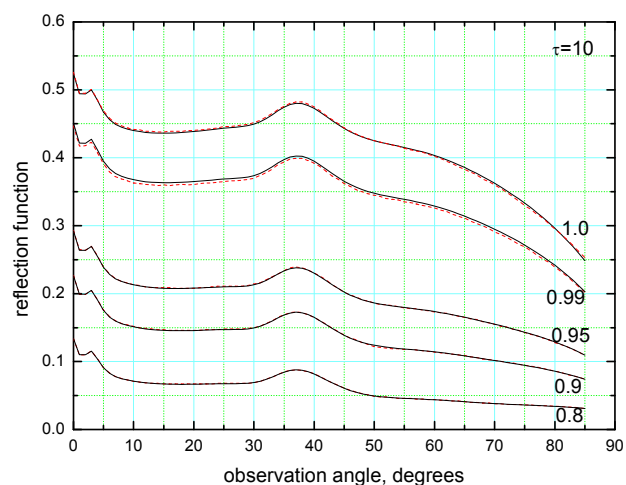


Fig. 8. Dependence of the reflection function on the incidence zenith angle for several values of the single scattering albedo and an optical thickness equal to 10. Exact results are given by black lines. Approximate results are given by red broken lines.

behave if the exact calculations are obtained for a different value of the effective radius as compared to that used in the preparation of LUTs. Therefore, Fig. 11 shows a comparison for the case of ω_0 equal to 0.95, 0.99 and 1.0 between exact results computed for an effective radius of $16\ \mu\text{m}$ and the approximations that are based on LUT values valid for an effective radius of $6\ \mu\text{m}$. It follows that the errors for non-absorbing clouds generally stay within 5%. They are somewhat larger in the vicinity of the rainbow and glory region. This is related to the fact that the position of the rainbow and also the angular positions of the glory rings are different for 6 and $16\ \mu\text{m}$ droplets. This problem will not arise for ice clouds because in this case, both rainbows and glories are absent. This can be seen in Fig. 12, which shows the comparison of the asymptotic results with exact calculations for ice clouds with fractal particles. The reflection functions of the

ice clouds are very smooth and do not have a glory or rainbow angular features. The different behavior between water and ice clouds in this angular region could be used for the cloud phase discrimination using, e.g., azimuthally scanning optical instruments. Generally, errors for ice clouds ($g=0.75$) are also small ($\leq 2\%$ for most of angles).

4 Conclusions

The accuracy of a number of analytical equations for cloud optical characteristics including reflection and transmission function over a reflective Lambertian ground has been studied. The asymptotic theory can be used for rapid estimations

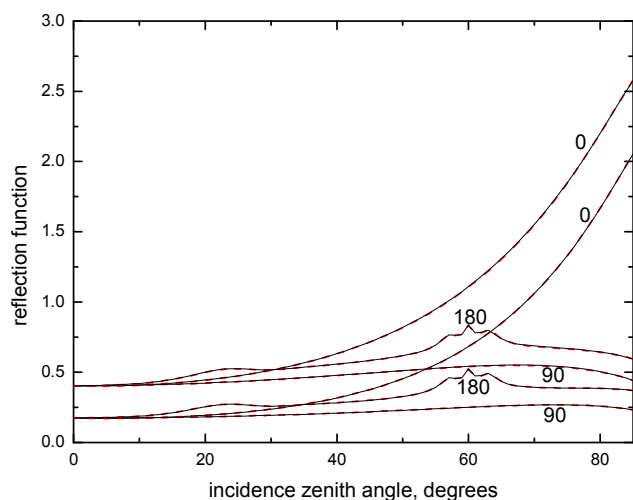


Fig. 9. Dependence of the reflection function on the incidence zenith angle for values of the single scattering albedo equal to 0.95 and 1.0, an optical thickness equal to 10, an observation angle of 60° and azimuth angles of 0° , 90° , and 180° . Lower lines correspond to the smaller values of ω_0 . Red broken lines show approximate results. Solid lines present exact radiative transfer calculations. The correspondent absolute value of the relative error $|\delta|$ is smaller than 0.5%.

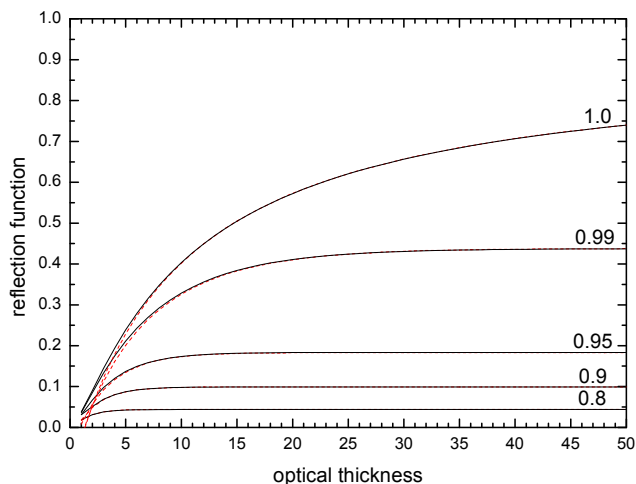


Fig. 10a. Dependence of the reflection function on the optical thickness for values of the single scattering albedo equal to 0.8, 0.9, 0.95, 0.99, 1.0, an observation angle of 0° and an incidence angle of 60° . Red broken lines show approximate results. Solid lines present exact radiative transfer calculations.

of the radiative characteristics in cloudy atmospheres. It is accurate for a cloud optical thickness $\tau \geq 5$ (and for some radiative transfer characteristics (see Fig. 4a) at $\tau \geq 3$). Only properties of optically thick water and ice clouds can be studied in the framework of the approximate theory discussed in this study.

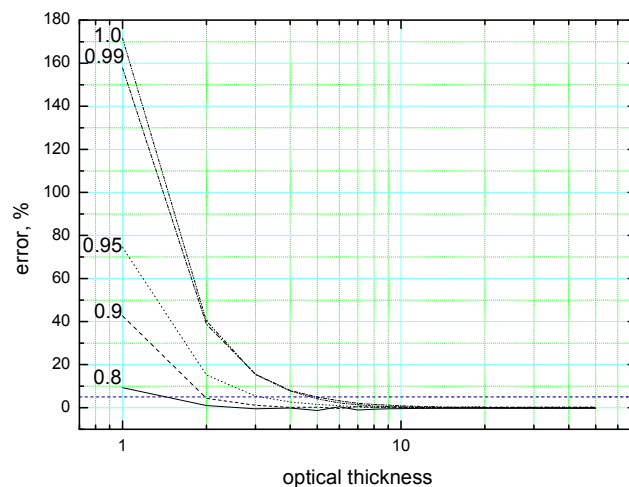


Fig. 10b. Dependence of the relative error on the optical thickness calculated using data shown in Fig. 10a for values of the single scattering albedo equal to 0.8, 0.9, 0.95, 0.99, 1.0.

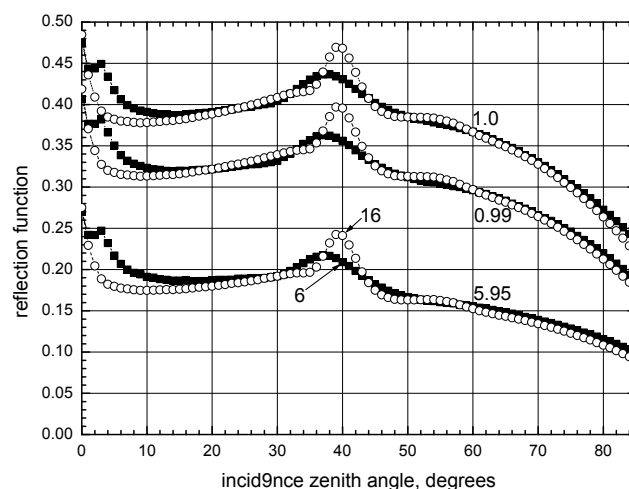


Fig. 11a. Dependence of the reflection function on the incidence zenith angle for values of the single scattering albedo equal to 0.95, 0.99 and 1.0, an observation angle of 0° and an incidence angle of 60° . Filled squares show approximate results. Circles give the results of the exact radiative transfer calculations. The increase of the error for the approximation in the rainbow and glory regions is due to the fact that LUTs for particles with an effective radius of $6 \mu\text{m}$ have been used to derive the approximate results. Exact calculations have been performed for an effective particle radius of $16 \mu\text{m}$. The asymmetry parameter ($g=0.8692$) has been the same for both calculations.

Asymptotic equations are very simple and can be used as a basis for the construction of high speed satellite cloud retrieval algorithms, which account for both multiple light scattering in a cloud and reflective properties of an underlying surface. They can be also used as a basis for the

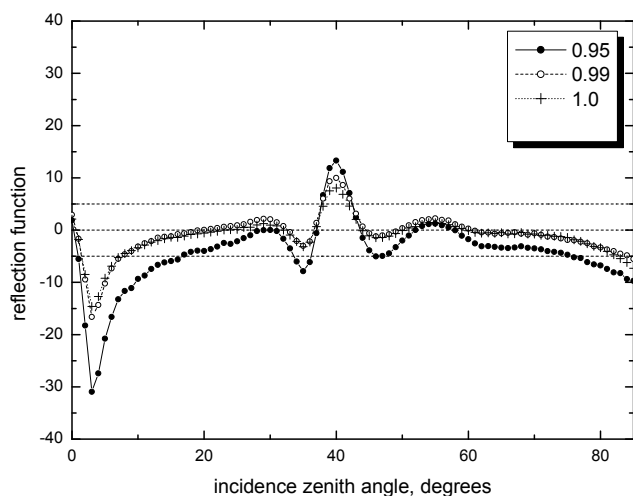


Fig. 11b. Dependence of the relative error on the incidence zenith angle calculated using data shown in Fig. 11a for values of the single scattering albedo equal to 0.95, 0.99 and 1.0.

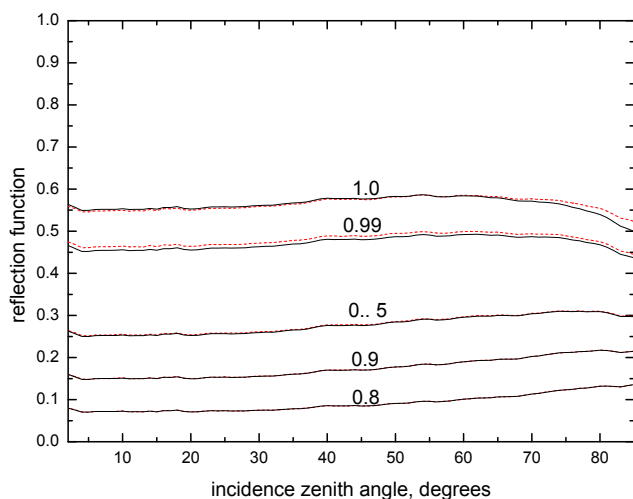


Fig. 12. Dependence of the reflection function on the incidence zenith angle for values of the single scattering albedo equal to 0.8, 0.9, 0.95, 0.99, and 1.0, an optical thickness equal to 10 and an observation angle of 0° . Red broken lines show approximate results. Solid lines represent exact radiative transfer calculations. The correspondent absolute value of the relative error $|\delta|$ is smaller than 2% at $\vartheta_0 \leq 75^\circ$. The fractal ice crystal phase function ($g=0.7524$) as described by Mishchenko et al. (1999) has been used in the calculations.

parameterization of cloud retrieval LUTs for the case $\tau \rightarrow \infty$. The correspondent errors (for the case of thick clouds) are smaller than the uncertainties in the forward models (e.g., the assumption of plane-parallel homogeneous clouds) and they are below calibration errors of optical instruments currently in orbit.

The accuracy of the equations presented is dependent on the characteristic in question. However, it is smaller than 5% for most of the studied cases relevant for the propagation of visible and near-infrared radiation in a cloudy atmosphere. Therefore, the equations could be used for the parameterization of radiative transfer blocks in global circulation and climate models, where even larger errors of approximations are commonly accepted due to computation time constraints and various other uncertainties inherent to atmospheric models.

The correspondent radiative transfer code CLOUD together with a user guide is available on line at <http://www.iup.physik.uni-bremen.de/~alexk>.

Acknowledgements. The authors would like to thank J. P. Burrows, V. V. Rozanov for their help and advice and W. M. F. Wauben as well as M. Mishchenko for providing the radiative transfer codes used for the computation of the LUTs. This work has been supported by the DFG Project DFG BU/688-2, the GLOWA-Danube project 97 GWK 04 “Rainfall Retrieval” and the Erich-Becker foundation (formerly Frankfurt Airport foundation), Germany.

Edited by: Q. Fu

References

- King, M. and Harshvardhan: Comparative accuracy of selected multiple scattering approximations, *J. Atmos. Sci.*, 44, 1734–1751, 1986.
- Kokhanovsky, A. A., Rozanov, V. V., Zege, E. P., Bovensmann, H., and Burrows, J. P.: A semi-analytical cloud retrieval algorithm using backscattered radiation in 0.4–2.4 μm spectral region, *J. Geophys. Res.*, 108, 4008, doi:10.1029/2001JD001543, 2003.
- Kokhanovsky, A. A.: *Cloud Optics*, Berlin: Springer-Verlag, 2006.
- Mishchenko, M. I., Dlugach, J. M., Yanovitskij, E. G., and Zakharova, N. T.: Bidirectional reflectance of flat, optically thick particulate layers: an efficient radiative transfer solution and applications to snow and soil surfaces, *J. Quant. Spectrosc. Radiat. Trans.*, 63, 409–432, 1999.
- Nakajima, T. and King, M. D.: Determination of the optical thickness and effective particle radius of clouds from reflected solar radiation measurements, Part 1. Theory, *J. Atmos. Sci.*, 47, 1878–1893, 1990.
- Rozanov, A. V., Rozanov, V., Buchwitz, M., Kokhanovsky, A., and Burrows, J. P.: SCIATRAN 2.0: a new radiative transfer model for geophysical applications in the 175–2400 nm spectral region, *Adv. in Space Res.*, 36, 1015–1019, 2005.
- van de Hulst, H. C.: The spherical albedo of a planet covered with a homogeneous cloud layer, *Astron. Astrophys.*, 35, 209–214, 1974.
- van de Hulst, H. C.: *Multiple Light Scattering: Tables, Formulas and Applications*, N.Y., Academic Press, 1980.
- Wauben, W. M. F.: *Multiple Scattering of Polarized Radiation in Planetary Atmospheres*, Ph.D. Thesis, Free University of Amsterdam, 1992.